Chapter 3

Faults and Novel Countermeasures for Optical Fiber Connections in Fiber-To-The-Home Networks

Mitsuru Kihara

Additional information is available at the end of the chapter

http://dx.doi.org/10.5772/54241

1. Introduction

The number of subscribers to broadband services in Japan now exceeds 34 million, and about 20 million were using fiber-to-the-home (FTTH) services in December 2011 [1]. The number of optical fiber cables continues to increase as the number of FTTH subscribers increases; however, unexpected faults have occurred along with this increase. One such fault is damage caused by wildlife including rodents, insects, and birds [2], and another is that caused by defective optical fiber connectors [3]. It is very important to detect and investigate the causes of these faults and to apply correct countermeasures.

The Technical Assistance and Support Center (TASC), Nippon Telegraph and Telephone (NTT) East Corporation is engaged in technical consultation and the analysis of optical fiber network faults for the NTT group in Japan and is contributing to eliminating the causes and reducing the number of faults in the optical fiber facilities of FTTH networks. The TASC has investigated and reported faults in various fiber connections using refractive index matching material with wide gaps between fiber ends and faults in fiber connectors with imperfect physical contact [4-6].

This chapter describes some of the faults with optical fiber connections in FTTH networks that the TASC has investigated. In addition, it introduces novel countermeasures for dealing with the faults. The various faults and countermeasures described in this chapter are shown in Fig. 1. First, section 2 briefly reviews a typical FTTH network and various fiber connections in Japan. Then section 3.1 reports faults with fiber connections that employ refractive index matching material. These faults have two major causes: One is a wide gap between fiber ends and the other is incorrectly cleaved fiber ends. Next, section 3.2 describes faults with fiber connections that employ physical contact (PC). This fault has the potential to occur when connector endfaces are contaminated. The characteristics of these faults are outlined. Novel countermeasures against the above-mentioned faults are introduced in section 4. In section 4.1, a new connection method using solid refractive index matching material is proposed as a countermeasure against faults caused by a wide gap between fiber ends. In section 4.2, a fiber optic Fabry-Perot interferometer based sensor is introduced as a way of detecting faults caused by incorrectly cleaved fiber ends. The sensor mainly uses laser diodes, an optical power meter, a 3-dB coupler, and an XY lateral adjustment fiber stage. In section 4.3, a novel tool for inspecting optical fiber ends is proposed as a countermeasure designed to detect faults caused both by incorrectly cleaved fiber ends and contaminated connector endfaces. The proposed tool has a simple structure and does not require focal adjustment. It can be used to inspect a fiber and clearly determine whether it has been cleaved correctly and whether the connector endfaces are contaminated or scratched. This chapter is summarized in section 5.

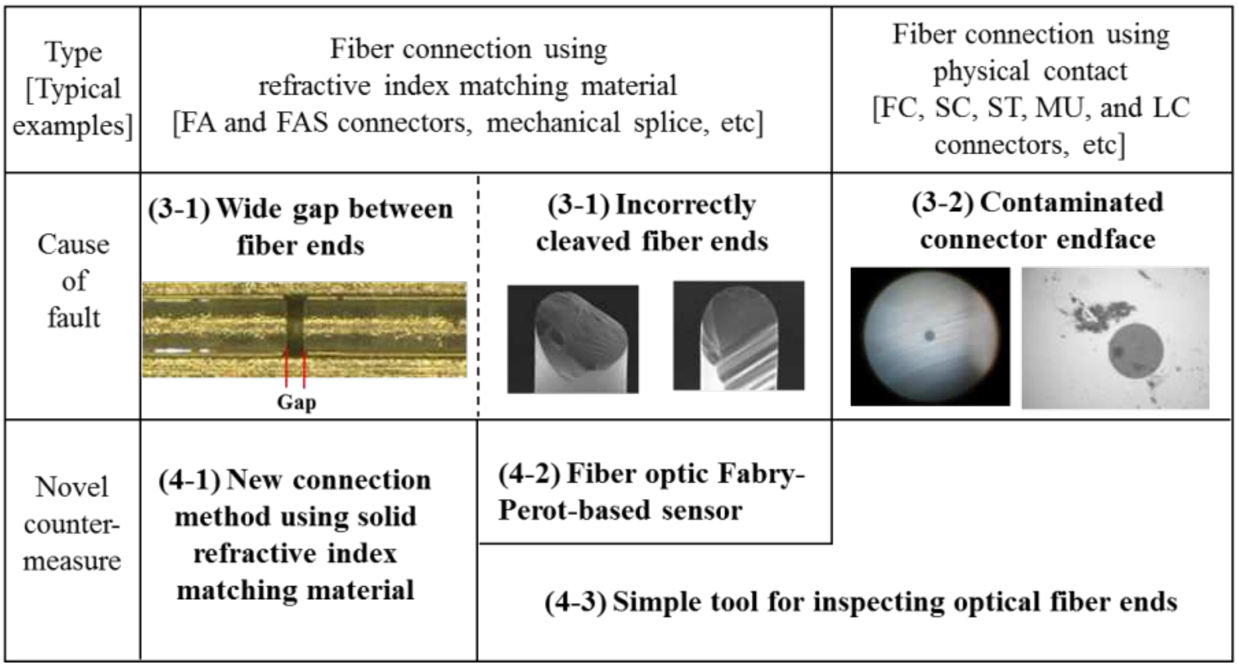

Figure 1. Various faults and their countermeasures dealt with in this chapter

2. Fiber-to-the-home network and various fiber connections

Figure 2 shows the configuration of a typical FTTH network in Japan, which is mainly composed of an optical line terminal (OLT) in a central office, underground and aerial optical fiber cables, and an optical network unit (ONU) inside a customer's home. The network requires various fiber connections at the central office, outdoors, and in homes. With the aerial and home-sited fiber connections in particular, field installable connectors or mechanical splices are used to make it possible to employ the most suitable wiring for the aerial condition and room arrangement. Field assembly (FA) termination connectors and field assembly small (FAS) connectors are types of field installable connectors [7-8].

In contrast, manufactured physical contact (PC)-type connectors, such as miniature-unit coupling optical fiber (MU) and single fiber coupling optical fiber (SC) connectors [9-10], are used in central offices and homes. These connectors require more frequent reconnection than field installable connectors.

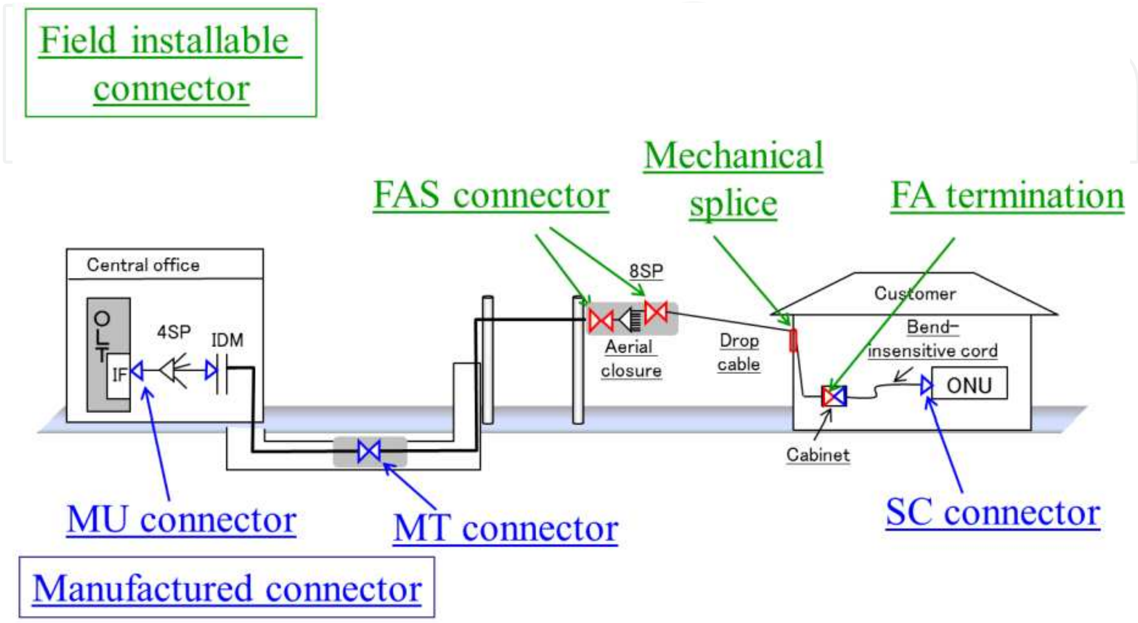

Figure 2. Typical FTTH network and various fiber connections

Figure 3(a) shows the basic structure of a PC-type connector, 3(b) shows that of a mechanical splice and 3(c) shows that of a field installable connector. With PC-type connectors, two ferrules are aligned in an alignment sleeve and connected using compressive force. Normally, two fiber ends in ferrules are connected without a gap and without offset or tilt misalignment. A mechanical splice is suitable for joining optical fibers simply in the field. It consists of a base with a V-groove guide, three coupling plates, and a clamp spring. When a wedge is inserted between the plates and the base, optical fibers can be inserted though the V-groove guide to connect and fix them in position by releasing the wedge between the plates and base [11]. Refractive index matching material is used to reduce Fresnel reflection. This connection procedure requires no electricity.

A field installable connector is composed of three main parts, a polished ferrule containing a short optical fiber (built-in optical fiber), a mechanical splicer, and a clamp. This connector holds the optical fiber drop cable or indoor cable sheath. To assemble the connection, the optical fiber end is cleaved and connected to the built-in optical fiber using a mechanical splice, and the cable sheath is fixed in the clamp. The structure allows connection to another optical fiber connector in the field. In addition, the field installable connector is fabricated based on the above-mentioned mechanical splice technique; therefore, the connection can be assembled without the use of special tools or electricity.

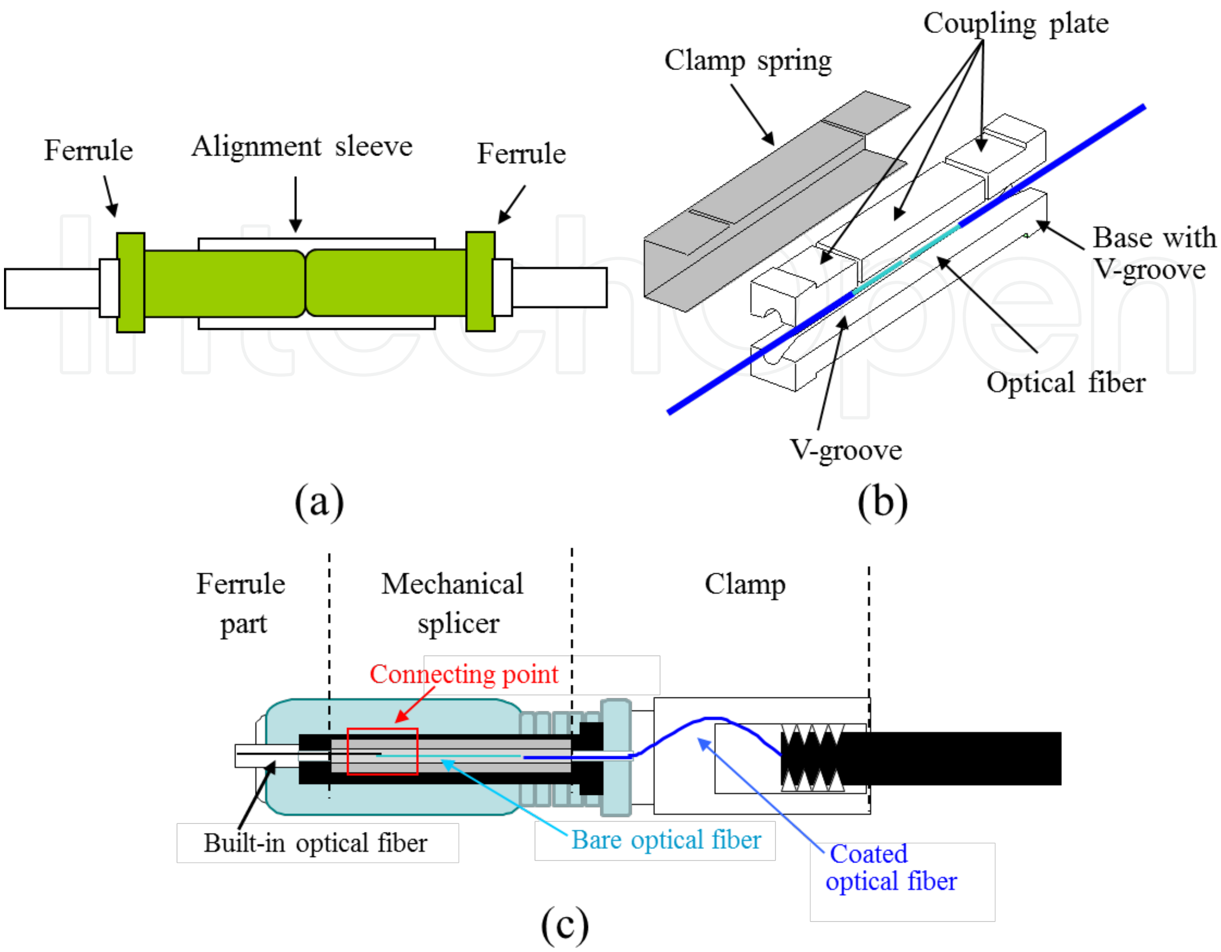

Figure 3. Basic structures of physical contact type connector, (b) mechanical splice, and (c) field installable connector

Both the mechanical splice and the field installable connector use the same fiber end preparation process before fiber installation. Figure 4 shows the fiber end preparation procedures. The coating of a fiber is stripped. Then the stripped fiber (bare fiber) is cleaned with alcohol, cut with a cleaver, inserted into the mechanical splice or the splicer inside a field installable connector, and joined to the opposite fiber or built-in fiber. Finally, the inserted fibers are fixed in position with a clamp. Stripping, cleaning, and cutting are important for successful fiber connection (to provide good performance) in the field. If any of these procedures are not conducted correctly, the performance of the fiber connection might deteriorate.

3. Faults with optical fiber connections

This section reports some of the faults with optical fiber connections in FTTH networks that the TASC has investigated. First, faults related to fiber connection using refractive index matching material are reported in section 3.1. Faults involving PC fiber connection are described in section 3.2.

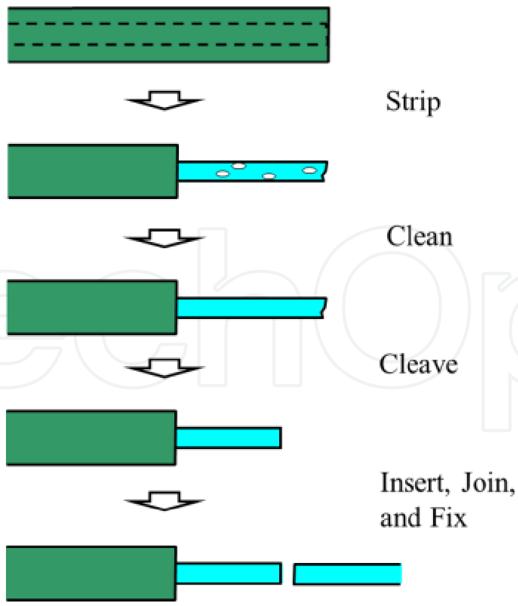

Figure 4. Optical fiber end preparation procedure

3.1. Fiber connection with refractive index matching material

There are two major causes of faults related to fiber connection using refractive index matching material: one is a wide gap between fiber ends and the other is an incorrectly cleaved fiber end. Figure 5 shows three connection models using refractive index matching material; (a) shows the normal connection state with a narrow gap between flat fiber ends, (b) shows an abnormal connection state with a wide gap between flat fiber ends, and (c) shows an abnormal state with an incorrectly cleaved (uneven) fiber end. With the normal connection (a), there is a very narrow (sub-micron) gap between the fiber ends because a normal fiber end is not completely flat. The very narrow gap is filled with silicone oil compound, which is used as the refractive index matching material in a normal connection. In the abnormal connection state (b) there is a very wide gap between the flat fiber ends, and the gap is not filled with refractive index matching material but is a mixed state consisting of refractive index matching material and air. In the abnormal connection state (c) there is a wide gap between flat and incorrectly cleaved (uneven) fiber ends. However, the gap between the fiber ends is filled with matching material.

The optical performance of various fiber connections using refractive index matching material was investigated experimentally. Wide gaps were formed between flat fiber ends by using MT connectors [12] and feeler gauges. A feeler gauge (thickness gauge tape) was installed and fixed in place between the two MT ferrules of a connector with a certain gap size by using a clamp spring. By changing the thickness of the feeler gauge, gaps of various sizes were obtained [13]. In contrast, incorrectly cleaved fiber ends were intentionally formed by adjusting the fiber cleaver so that the bend radius would be too small [14]. The cracks in these incorrectly cleaved fiber ends were from 30 to 200 μm in the axial direction. Using these incorrectly cleaved fiber ends, we fabricated field installable connectors as experimental samples. The fabricated

MT connector with a feeler gauge and field installable connector samples were subjected to a heat-cycle test in accordance with IEC 61300-2-22 (-40 to 70°C, 10 cycles, 6 h/cycle) to simulate conditions in the field. The insertion and return losses were measured.

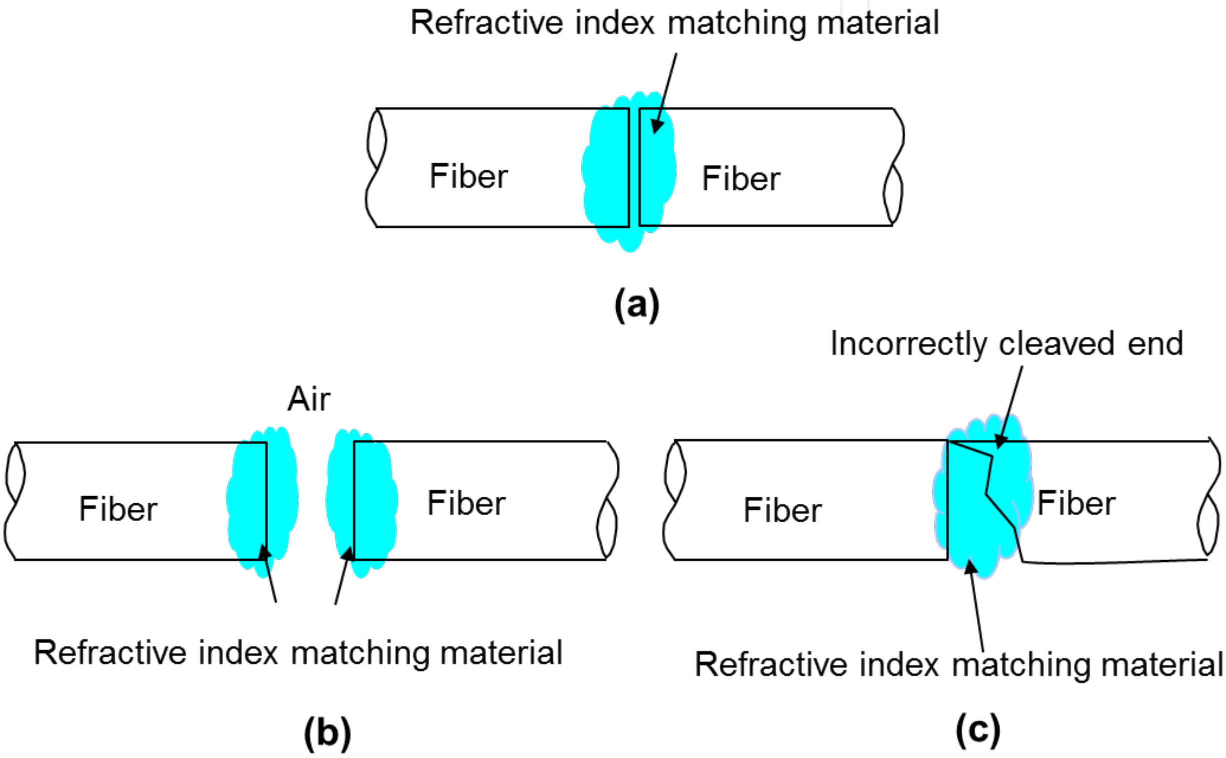

Figure 5. Fiber connection models using refractive index matching material: (a) normal connection with narrow gap between flat fiber ends, (b) abnormal connection with wide gap between flat fiber ends, and (c) abnormal connection with an incorrectly cleaved (uneven) fiber end

The insertion and return losses of an abnormal connection sample with a wide gap between flat fiber ends are shown in Fig. 6. The optical performance changed and was unstable. The insertion loss was initially 2.7 dB and then varied when the temperature changed. The maximum insertion loss exceeded 30 dB. The return losses also varied from 20 dB to more than 60 dB. This performance deterioration is thought to be caused by the mixture of refractive index matching material and air-filled gaps between the fiber ends in the MT connector sample.

Refractive index matching material moved in the gap when the temperature changed, and the mixed state change of the refractive index matching material and the air between the fiber ends induced the change in optical performance. When there is a mixed state consisting of refractive index matching material and air between the fiber ends, the boundary between the refractive index matching material and air could be uneven. In this state, the transmitted light spread randomly in every direction at the boundary. Therefore, the insertion loss increased to more than 30 dB. Consequently, the optical performance of fiber connections with a wide gap between flat fiber ends might be extremely unstable and vary widely. Therefore, it is important to prevent the gap from becoming wider and avoid mixing air with the refractive index matching material in the gap between fiber ends for these fiber connections.

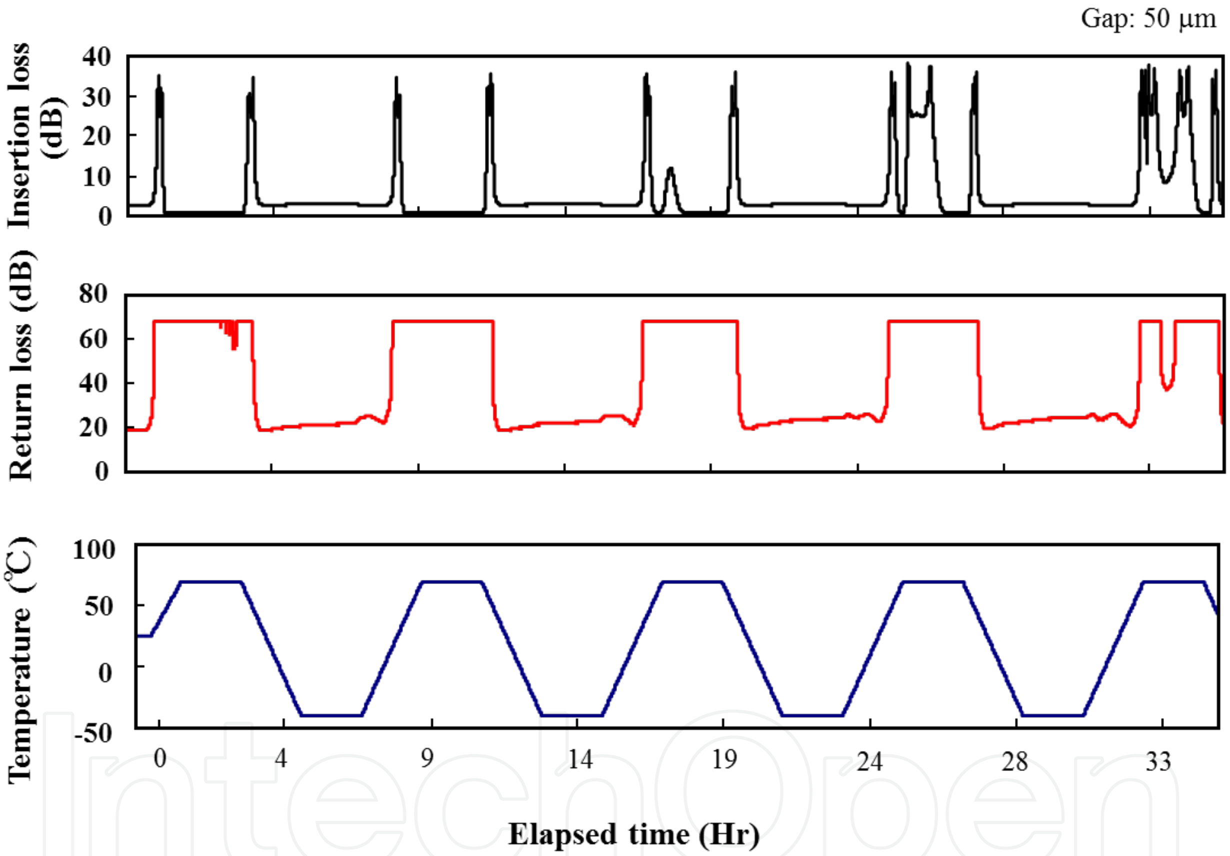

Figure 6. Heat-cycle test results for fiber connection with wide gap between flat fiber ends

The insertion and return losses of an abnormal connection sample with an incorrectly cleaved (uneven) fiber end also changed greatly and were unstable. Figure 7 shows a scatter diagram plotted from the measured insertion and return loss values to enable the values to be easily and simultaneously understood. The horizontal lines indicate insertion loss and the vertical lines indicate return loss. The scatter diagram plots minute insertion and return losses that occurred during the heat cycle test. There are both huge vertical and horizontal fluctuations in the plotted data in Fig. 7. The insertion and return loss values changed periodically during temperature cycles. The initial insertion loss was low at about 1 dB and the initial return loss was high at more than 40 dB. The insertion loss increased greatly and then the return loss decreased as the temperature changed. At worst, the insertion loss changed to 43 dB and the return loss changed to 28 dB.

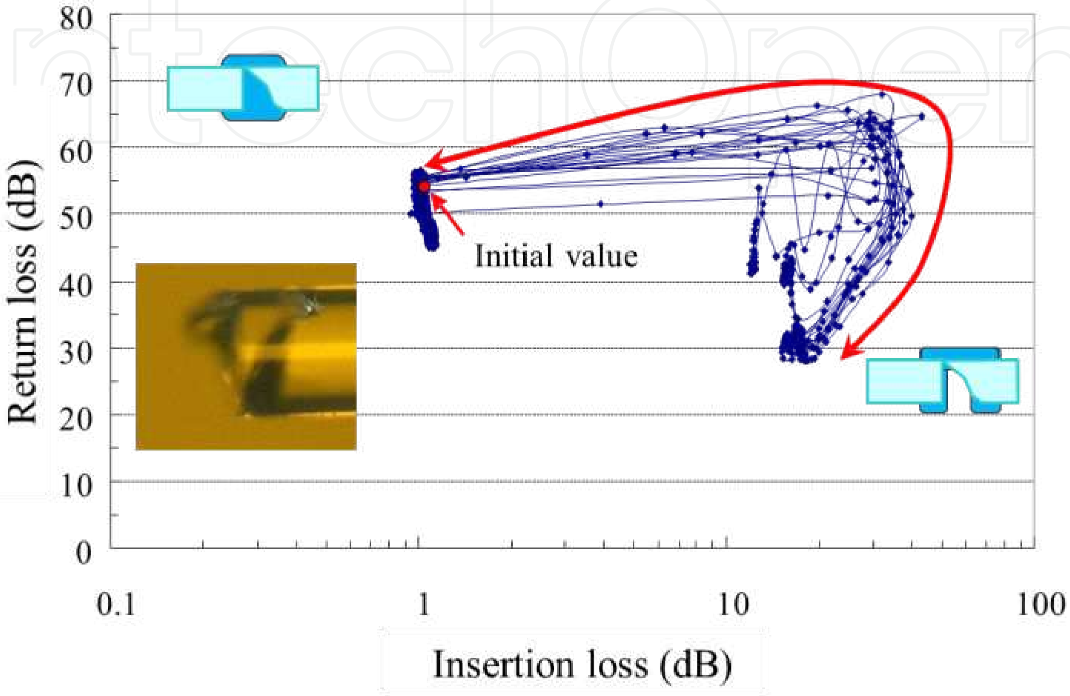

Figure 7. Scatter diagrams of results from heat cycle test for fiber connection with an incorrectly cleaved (uneven) fiber end

The great changes in the insertion and return losses are also attributed to a partially air-filled gap. The gap was not completely filled with refractive index matching material and thus consisted of a mixed state of refractive index matching material and air because of the incorrectly cleaved fiber ends. The boundary between the refractive index matching material and air could be uneven. The transmitted light in this state spread randomly in every direction at the boundary. Therefore, the insertion and return losses became much worse. When the gap was filled with refractive index matching material and there was no air, the optical performance was not so bad. When the gap was a mixed state of refractive index matching material and air, the optical performance deteriorated. The connection state is thought to vary with temperature. These results suggest that the insertion and return losses of fiber connections using incorrectly cleaved fiber ends might change to, at worst, more than 40 dB for the former and less than 30 dB for the latter. Consequently, it is important to prevent gaps between the correctly and incorrectly cleaved ends of fiber connections from becoming wider, and air from mixing with the refractive index matching material in the gaps. Therefore, incorrectly cleaved fiber ends must not be used. An effective countermeasure is to check the fiber ends cleaved with fiber cleavers. Reference [6] is recommended to those readers requiring a more detailed analysis of these abnormal connection states.

3.2. Physical Contact (PC) type connector

This section discusses the deterioration in optical performance caused by the contamination of manufactured physical contact (PC)-type connectors. It has been reported that contamination on a PC-type connector may significantly degrade the performance of mated connectors [15-17]. In this report, contamination was found on the connector endface and the sides of the connector ferrule. To study the effect of contamination on the optical performance of mated connectors, various connection conditions for PC-type connectors in abnormal states are discussed. The abnormal connection conditions are shown in Fig. 8. With PC-type connectors, two ferrules are aligned in an alignment sleeve and connected using compressive force. Normally, two fiber ends in ferrules are connected without a gap and without offset or tilt misalignment. However, if contamination is present, the connection state might become abnormal. An abnormal state can be induced by four conditions: (A) light-blocking caused by contamination on the fiber core, (B) an air-filled gap caused by contamination, (C) tilt misalignment caused by contamination, and (D) offset misalignment caused by contamination. Conditions (A) to (C) are caused by contamination on the ferrule endface. Conditions (C) and (D) are caused by contamination on the side of the ferrule. The performance deterioration caused by contamination (abnormal state) is calculated using the ratio of core contamination coverage and the Marcuse equations [18]. Figure 9 shows the individual calculated insertion losses for the four abnormal conditions. In condition (A), as the core contamination coverage ratio increases, the insertion loss increases. When the ratios are 0.5 and 0.8, the insertion losses are 3 and 7 dB, respectively. This connection condition could degrade the return loss due to the difference between the refractive indices of the fiber core and contamination. Condition (B) may be caused by contamination on the ferrule endface or fiber cladding. As the gap width becomes larger, the calculated insertion loss increases. The insertion loss caused by an air-filled gap is dependent on wavelength. When the wavelengths are 1.31 and 1.55 μm, the insertion losses of a 50-μm gap are 1.0 and 0.4 dB, respectively. This connection condition could also degrade the return loss caused by the difference in the refractive index between the fiber core and air [19]. Condition (C) may be caused by contamination on the edge of the ferrule endface and on the side of the ferrule. As the tilt angle increases, the calculated insertion loss increases. The insertion loss caused by tilt misalignment is dependent on wavelength. When the wavelengths are 1.31 and 1.55 μm, the insertion losses for a 3º misalignment angle are 1.4 and 1.3 dB, respectively. This connection condition might also have a detrimental effect on the return loss due to the difference between the refractive indices of the fiber core and air. Condition (D) may be caused by contamination on the side of the ferrule. When the offset is larger, the calculated insertion loss is higher. The insertion loss caused by offset misalignment is also dependent on wavelength. When the wavelengths are 1.31 and 1.55 μm, the insertion losses of a 3-μm offset are 1.9 and 1.5 dB, respectively. Current PC-type connectors usually have a small clearance between the outer diameter of the ferrule and inner diameter of the alignment sleeve. Therefore, the offset and tilt angle cannot be so large that the insertion losses become low. Conditions (A) and (B), which are caused by contamination on the fiber and ferrule endfaces, are thought to mainly affect the optical performance of connectors.

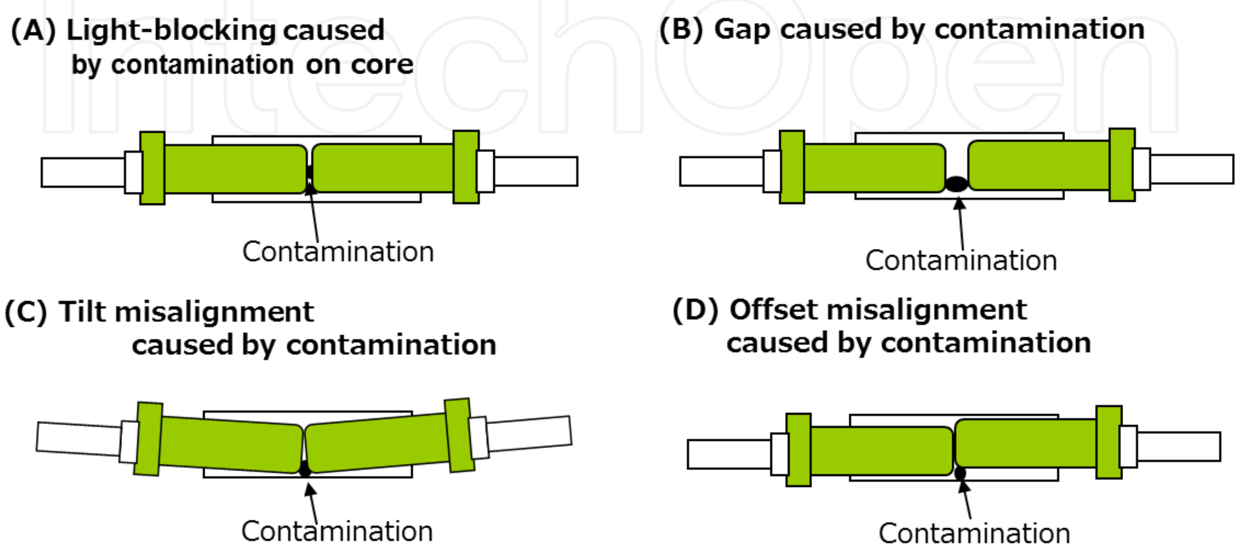

Figure 8. Abnormal connection states for PC type connector with contamination

Faults with PC-type connectors caused by contamination were investigated experimentally. Figure 10 shows examples of the investigated connectors. Figure 10 (a) is a normal sample (no contamination on the connector ferrule endface), and (b) to (e) are samples with contamination on the connector ferrule endface. The insertion losses at 1.31 and 1.55 μm were both 0.1 dB and the return loss at 1.55 μm was 58 dB for the uncontaminated sample. This optical performance is good and satisfies the required specifications for an SC connector. However, with the contaminated ferrule endfaces of samples (b) to (d), the insertion losses varied and exceeded 0.5 dB. The return losses were less than 40 dB. This optical performance does not satisfy the specifications for an SC connector. The losses with samples (b) and (c) are thought to be due to condition (A), and the loss with sample (d) is thought to be due to condition (B). With contamination sample (e), the optical performance was not bad and satisfied the SC connector specifications. Consequently, if there is contamination on a PC-type connector, the performance might deteriorate. An effective countermeasure against the loss increase caused by contamination is to inspect the PC-type connector endface prior to connection. When the connector endface is contaminated it must be cleaned with a special cleaner [20]. The countermeasures against connector endface contamination and incorrect cleaving are effective in reducing connector faults.

http://dx.doi.org/10.5772/54241

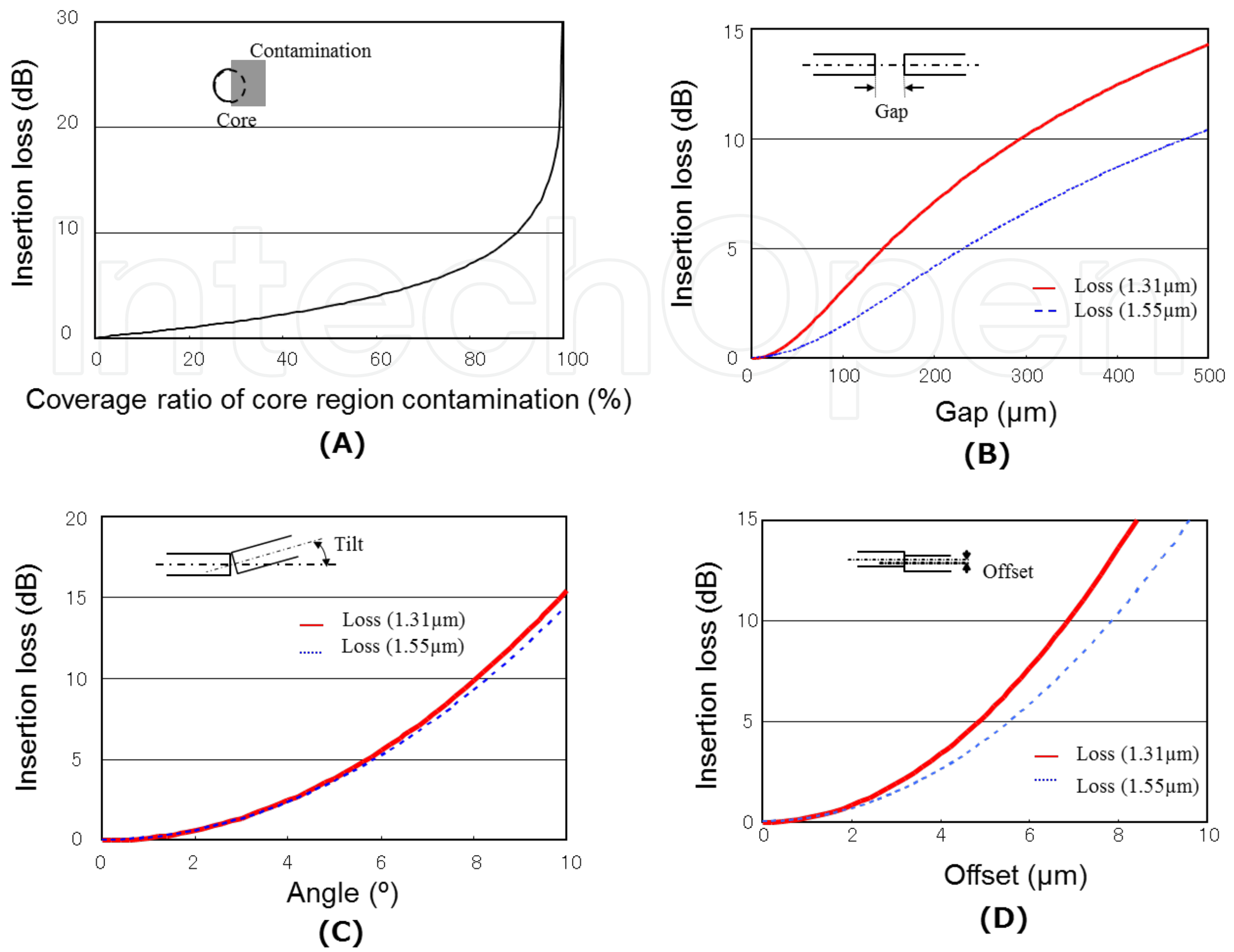

Figure 9. Calculated insertion loss, (A) cover ratio of contamination to fiber core, (B) caused by air-filled gap, (C) caused by tilt, and (D) caused by offset

4. Novel countermeasures

This section introduces novel countermeasures designed to deal with the faults described above. In section 4.1, a new connection method using solid refractive index matching material is proposed as a way of dealing faults caused by wide gaps between fiber ends. In section 4.2, a fiber optic Fabry-Perot interferometer based sensor is introduced as a countermeasure designed to prevent faults caused by incorrectly cleaved fiber ends. In section 4.3, a novel tool for inspecting optical fiber ends is proposed as a technique for detecting both faults caused by incorrectly cleaved fiber ends and those caused by contaminated connector endfaces.

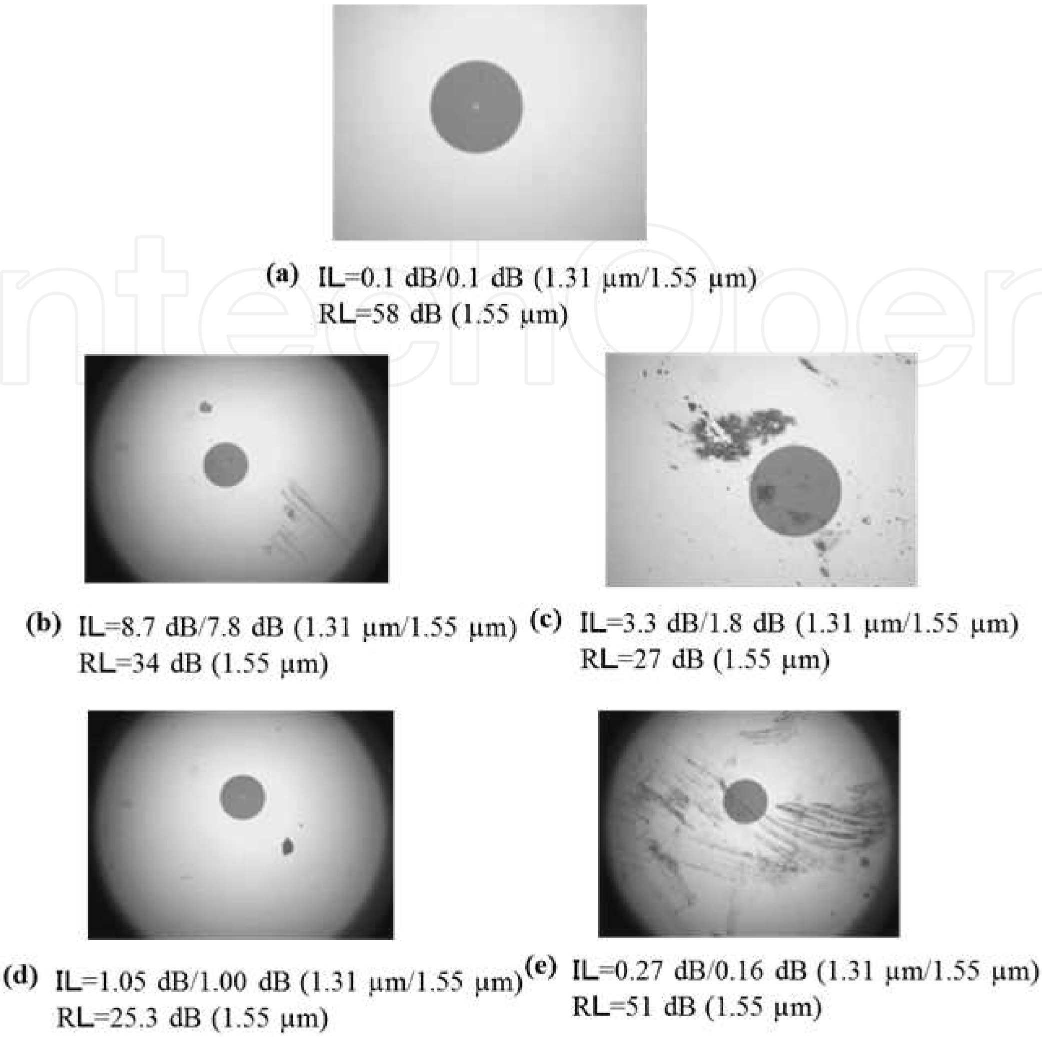

Figure 10. Examples of contamination on connector endface, (a) uncontaminated connector endface, and (b-e) different contaminations on connector endface

4.1. New connection method using solid refractive index matching material

The optical performance of fiber connections with a wide gap between flat fiber ends might be extremely unstable and vary widely. This performance deterioration may not occur immediately after installation but intermittently over time. In the event of an unusual fault, it is difficult to find the defective connection, and it takes long time to repair the fault. Therefore, it is important to prevent the gap between fiber ends from becoming wider in joints that employ refractive index matching material. A novel optical fiber connection method that uses a solid resin as refractive index matching material has been proposed [21]. The new connection method provides a high insertion loss that exceeds the loss budget between network devices when there is a wide gap between fiber ends (defective connection) and a suitable low insertion loss when the gap is less than a par-

http://dx.doi.org/10.5772/54241

ticular width (normal connection). The experimental optical performance of the proposed connection method is also discussed in this section.

The following two points are important as regards the new refractive index matching material.

i. An elastic solid resin must be used that has almost the same refractive index as the fiber core.

ii. Refractive index matching material with a particular width should be inserted between fiber ends (A and B) and tilted at a special tilt angle to the optical axis of the fiber.

The refractive index matching material must maintain its shape; therefore, a solid resin is used since the connection state cannot be easily changed. Figure 11(a) and (b) show the principles of this connection method. The incident light is refracted at the boundary surface of the refractive index matching material when the fiber ends do not touch it (there is a wide gap between the fiber ends, as shown in Fig. 11(a)). In this case, there is a high insertion loss because of the offset misalignment. In contrast, the incident light will travel straight into the refractive index matching material when it is touched by both fiber ends (the gap between the fiber ends is less than a particular width, as shown in Fig. 11(b)). The insertion loss in Fig. 11(b) is much lower than that in Fig. 11(a).

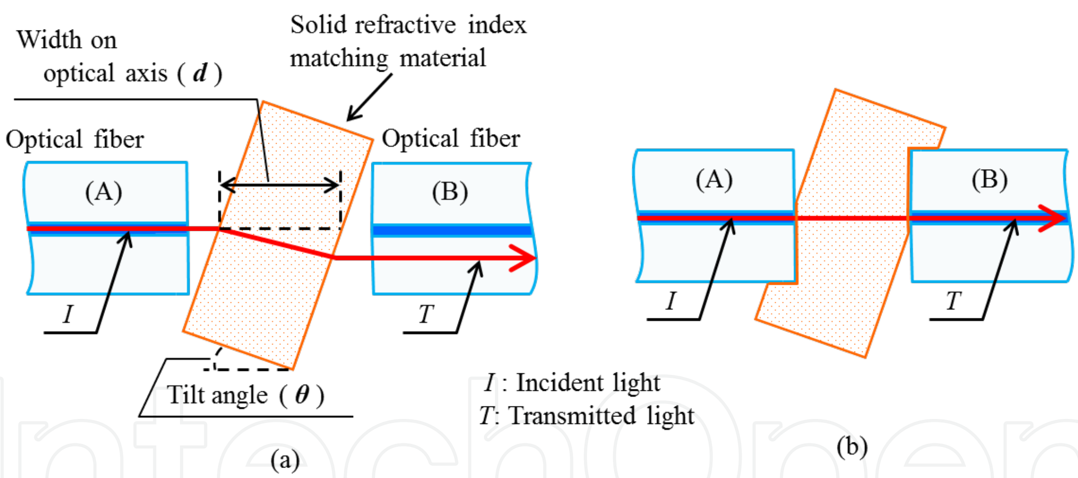

Figure 11. Proposed connection method: (a) fiber ends do not touch matching material, and (b) fiber ends touch matching material

A connection method using solid refractive index matching material based on the above-mentioned considerations was designed and used in the following procedure.

First, a target low insertion loss was set when the gap was narrower than a particular width d and then the particular width of the solid matching material on the optical axis of the fiber was determined.

Then the target high insertion loss was set when the gap was a wider than a particular width d and a special tilt angle θ was determined for the solid refractive index matching material.

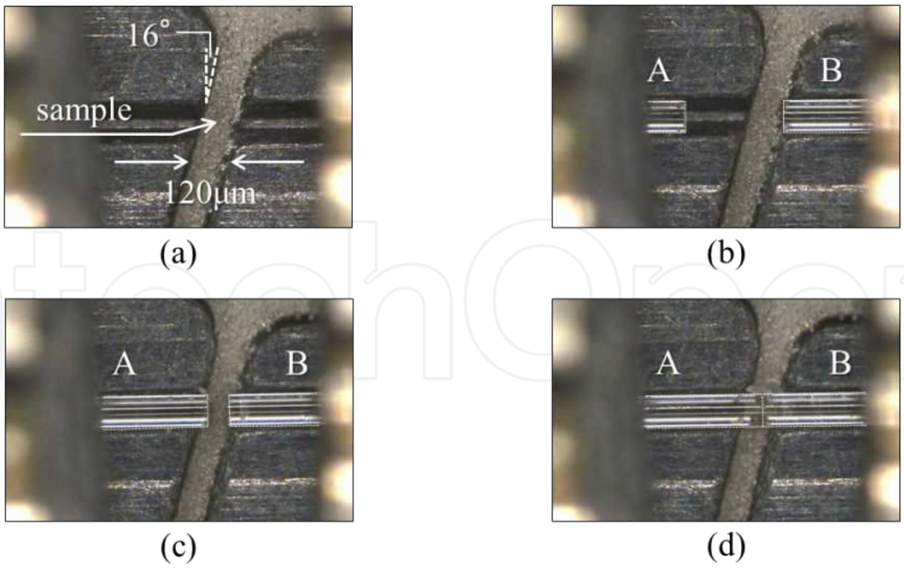

Figure 12. Composition of experimental conditions: (a) V-grooved substrate and sample, (b) fiber A does not touch sample, (c) fiber A just touches sample, and (d) fiber A is close to fiber B and very narrow gap is filled with sample

In step 1, the insertion loss caused by the gap between the fiber ends was calculated by using a Marcuse equation [18]. The insertion loss should be less than 0.5 dB to satisfy the mechanical splice specifications. However, when the insertion loss was 0.5 dB, d was 60 μm, which was too small to handle the refractive index matching material. Therefore, the target d was doubled to 120 μm. The insertion loss then became 2 dB.

In step 2, the insertion loss caused by the misalignment of the offset was calculated by using another Marcuse equation [3]. Another target insertion loss of 20 dB was determined in order to exceed the loss budget between network devices. The insertion loss became 20 dB when θ was 16°.

A sample made of the solid refractive index matching material (silicone resin) was fabricated based on the above parameters. Experiments were carried out with mechanical splices and samples of solid matching material. A groove was dug with the same shape as the sample, and the sample was tilted at 16° to the optical axis of the fiber, as shown in Fig. 12(a). A state was maintained whereby fiber end B always touched the sample, and fiber end A gradually moved toward the sample (Fig. 12(b)-(d)). The insertion and return losses were measured for different gap widths. Figure 12(b) shows the state in which fiber end A did not touch the sample. Figure 12(c) shows the state where fiber end A just touched the sample, and fiber end A was close to fiber end B, and Fig. 12(d) shows the state where the very narrow gap between the fiber ends was filled by the sample.

Figure 13(a) and (b) show the insertion and return loss results at wavelengths of 1.31 and 1.55 μm, respectively. When fiber end A did not touch the sample, the insertion loss always exceeded 20 dB. Moreover, the return losses were constant at 15 dB. When fiber end A just touched the sample, the insertion losses decreased to 2.5 and 2.3 dB, and the return losses increased to 51.7 and 48.6 dB at wavelengths of 1.31 and 1.55 μm, respectively. In addition, when fiber end A was close to fiber end B and the very narrow gap between fiber ends was filled by the sample, both insertion losses decreased to around 0.1 dB, and the return losses were 53.4 and 45.5 dB at wavelengths of 1.31 and 1.55 μm, respectively. These experimental results were consistent with the target values based on the design. If there is a defective connection that has a wide gap, the insertion loss can always be extremely high. In this case, communication services may be immobilized. With the connection method, engineers can detect the defective connection immediately after installation.

Consequently, a new connection method using solid refractive index matching material is proposed as a countermeasure against faults caused by a wide gap between fiber ends. This connection method can provide insertion losses of more than 20 dB or less than 2 dB, respectively, when the gap between the fiber ends is more or less than 120 μm.

4.2. Fiber optic fabry-perot interferometer based sensor

Field installable connections that have incorrectly cleaved fiber ends might lead to insertion losses of more than 40 dB induced by temperature changes, which may eventually result in faults in the optical networks. Therefore, it is important to use correctly cleaved fiber ends to prevent network failures caused by improper optical fiber connections. This means that we need a technique for inspecting cleaved optical fiber ends.

Cleaved optical fiber ends are usually inspected before fusion splicing with a CCD camera and a video monitor installed in fusion splice machines [22]. On the other hand, cleaved optical fiber ends are not usually inspected when mechanical splices and field installable connectors are assembled. These connections are easy to assemble and does not require electric power. Therefore, an inspection method is needed for these connections. A fiber optic Fabry-Perot interferometer based sensor for inspecting cleaved optical fiber ends has been proposed [23-24].

The basic concept of the proposed sensor for inspecting cleaved optical fiber ends is shown in Fig. 14. Figure 14(a) and (b), respectively, show fiber connections in which a fiber with a flattened end for detection is used in the inspection of incorrectly cleaved (uneven) and correctly cleaved (flat) fiber ends. The ratio of the reflected light power (P_r or P_r') to the incident light power (P_i or P_i') within each connection is measured. Two optical fibers are connected with an air gap S remaining between them. Misalignments of the offset and tilt between the fibers and the mode field mismatch are not taken into account. Under both conditions, Fresnel reflections occur at the fiber ends because of refractive discontinuity. In Fig. 14(a), the reflected light from the uneven end spreads in every direction, and the back-reflection efficiency ratio, P_r/P_i, is determined using the Fresnel reflection at the fiber end for detection in air. The Fresnel reflection R_0 is defined by the following equation.

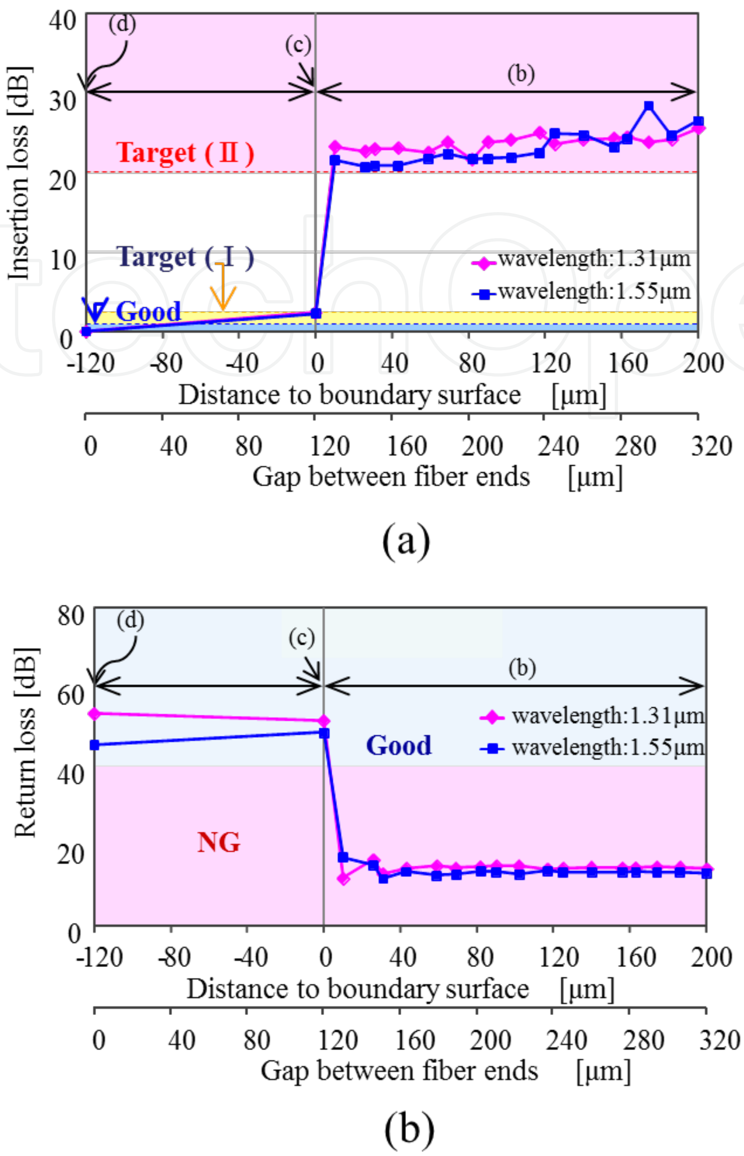

Figure 13. Results of (a) insertion loss and (b) return loss

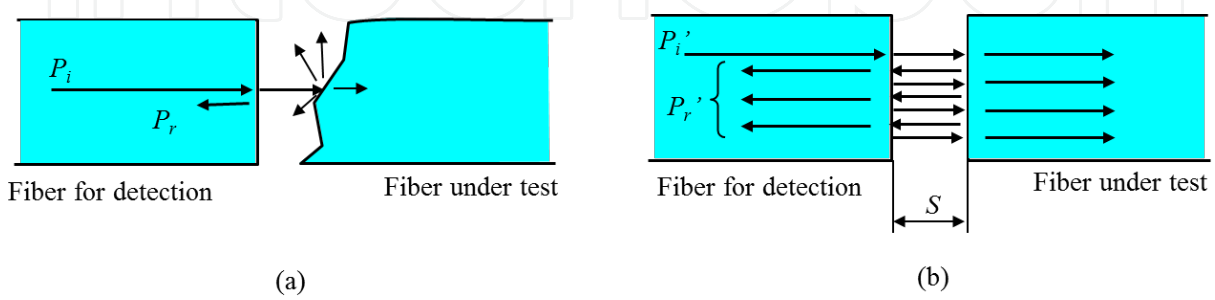

Figure 14. Basic concept of proposed sensor: (a) inspecting uneven fiber end, and (b) inspecting flat fiber end

$$R_0 = \left(\frac{n_1 - n}{n_1 + n} \right)^2 \tag{1}$$

Here n_1 and n denote the refractive indices of the fiber core and air, respectively.

In Fig. 14(b), some of the incident light is multiply reflected in the gap. The phase of the multiply reflected light changes whenever it is reflected, which interferes with the back-reflected light at the optical fiber connection. These multiple reflections between fiber ends are considered to behave like a Fabry-Perot interferometer [25-27]. Two flat fiber ends make up a Fabry-Perot interferometer. Based on the model, the returned efficiency R (= P_r'/P_i') is defined by the following equation.

$$R = \frac{4R_0 \sin^2(2\pi nS / \lambda)}{(1 - R_0)^2 + 4R_0 \sin^2(2\pi nS / \lambda)} \tag{2}$$

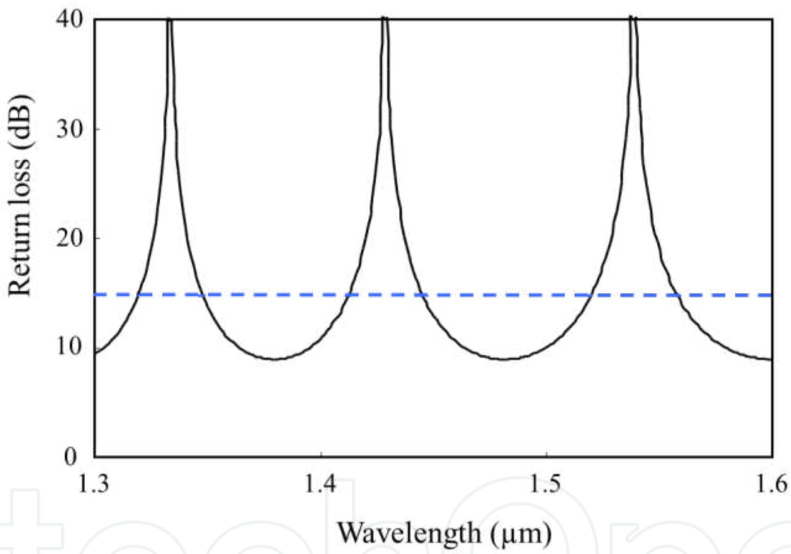

Figure 15. Return losses from uneven (dashed line) and flat (solid line) fiber ends

The return losses in dB are derived by multiplying the log of the reflection functions by -10. Here S and λ denote the gap size and wavelength, respectively. According to Equation (2), the return loss depends on S and λ. Figure 15 shows the calculated return losses from the uneven (incorrectly cleaved) and flat (correctly cleaved) fiber ends. The dashed and solid lines in the figure represent the calculations for the uneven and flat ends based on Equations (1) and (2), respectively. Here, the refractive indices n_1 and n were 1.454 and 1.0, and the gap size used for Equation (2) was 10 μm. The return losses of the uneven end were independent of wavelength and had a constant value of 14.7 dB. The return losses of the flat end varied greatly and periodically and resulted in a worst value of ~8.7 dB because of the Fabry-Perot interference.

The return loss values at wavelengths of 1.31 and 1.55 μm were 11.2 and 18.9 dB, respectively. Even if the gap size and wavelength period were changed, the return losses varied as greatly as the values at a 10-μm gap [28]. These results indicate that an inspected fiber end can be considered uneven or flat depending on whether or not the measured return losses from the fiber end at two wavelengths are both ~14.7 dB.

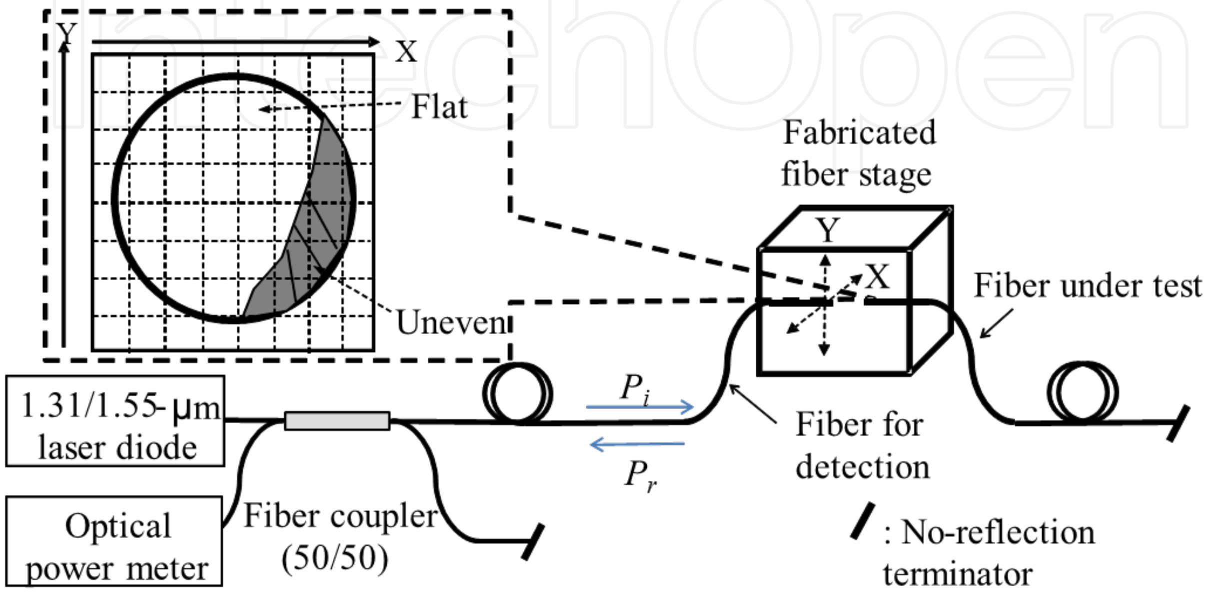

Figure 16. Experimental setup including fiber stage

Based on the above principle, we have designed the inspection sensor shown in Fig. 16. This sensor is composed of two light sources emitting at different wavelengths, an optical power meter, an optical coupler, and a fiber stage. In this proposed sensor, one light source is turned on and the other is turned off. The return loss values are measured separately at two wavelengths. The fiber stage is the most important component because a Fabry-Perot interferometer must be created in it by the fiber for detection and the fiber under test. The other equipment can be adapted from commercially available devices. Therefore, we fabricated a new fiber stage with the following characteristics to implement the proposed technique, as shown in Fig. 17. The dimensions of the fabricated fiber stage are 90 x 100 x 110 mm, which is small enough to be portable in the field. It is also suitable for operation in an outside environment because it does not require a power source. Manual driving was adopted for moving the fiber ends. Two V-grooves for the alignment of two fiber ends were used to create a Fabry–Perot interferometer. These two V-grooves were originally one V-groove that was divided into two. By using the same V-groove for alignment, any tilting of the two fibers along their Z-axes can be reduced. The X- and Y-axes for the scanning direction of the fiber ends were chosen from several alternatives, the direction of the radius, spirally, or with one stroke, due to the streamlining of the fiber stage mechanism. The minimum distance the V-groove can move was designed to be 10 μm along both the X- and Y-axes. The stage was designed to move along both the X- and Y-axes to a maximum distance of 250 μm to cover the entire end of 125-μm-diameter fibers.

http://dx.doi.org/10.5772/54241

Two levers are provided for manually operating only the left V-groove. The left lever moves the left V-groove along the Y-axis at 10 μm per pitch up to a maximum distance of 250 μm. Similarly, the right lever moves the left V-groove along the X-axis at 10 μm per pitch up to a maximum distance of 250 μm.

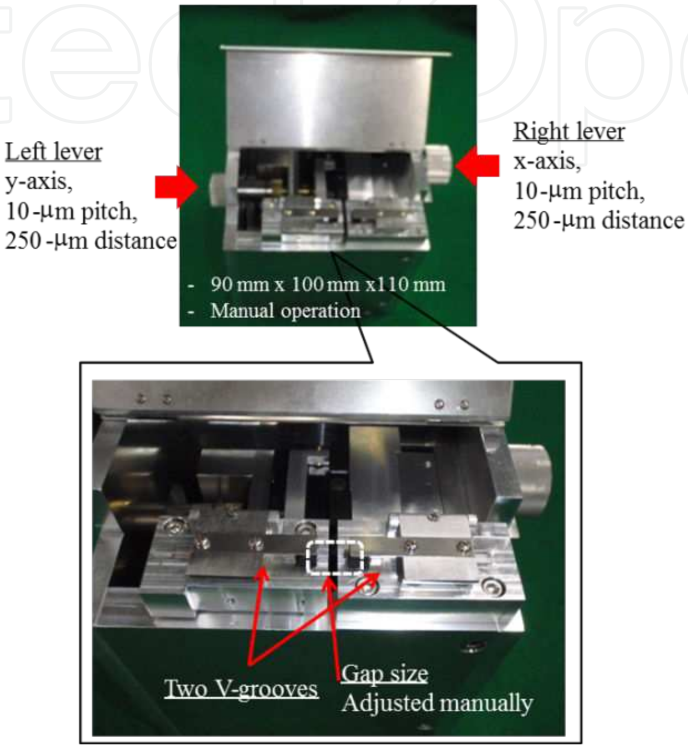

Figure 17. Fabricated fiber stage

In the experiments, the gap between the fiber for detection and the fiber under test was set at 40 μm, and each scanning distance was set at 10 μm. Typical experimental results are shown in Fig. 18. In the figure, (a) and (c) show the flat parts of the inspected fiber end found using the proposed inspection sensor and (b) and (d) show SEM images of the flat end. The fiber ends seen in Fig. 18(a) and (c) were found to be correctly and incorrectly cleaved, respectively. The experimental image with a correctly cleaved fiber end shows that the flat parts form a circle with a diameter of about 140 μm, which is slightly larger than the actual 125-μm-diameter fiber end. This is because the mode field area of light may radiate from the fiber end for detection. In contrast, the experimental results for the incorrectly cleaved fiber end show that half the fiber end parts are flat and half are uneven. The results obtained with the proposed inspection method and those obtained by SEM observation are in good agreement.

The above results show that the proposed sensor made it possible to determine accurately whether the fiber ends were correctly or incorrectly cleaved for all the samples examined. Since the proposed sensor for cleaved optical fiber ends is based on the Fabry-Perot interferometer and a new fiber stage, it allows us to determine whether 10 x 10 μm areas of a cleaved optical fiber end are flat or uneven. The measured results of the inspected flat and uneven fiber ends were in good agreement with those obtained using an SEM.

4.3. Simple tool for inspecting optical fiber ends

The conventional inspection method for a cleaved fiber end involves checking it regularly (about once a week) to ensure good cleaving quality by using a CCD camera and the video monitor of a fusion splicer. If the cleaved fiber end is imperfect, first the fiber cleaver blade is replaced. If no improvements result from this countermeasure, the fiber cleaver itself must be repaired by the manufacturer. In contrast, the conventional inspection method for optical fiber connector endfaces is to check the surface before connecting the mated connector. This method uses a CCD camera and the video monitor of a specialized piece of inspection equipment [29]. If the connector endface is contaminated, it must be cleaned with a special cleaner. These methods using a CCD camera and a video monitor are expensive and unsuitable for use with straightforward fiber connections in the field. Therefore, a simple and economical inspection tool for cleaved fiber ends and connector endfaces suitable for use in the field have been proposed [30-31].

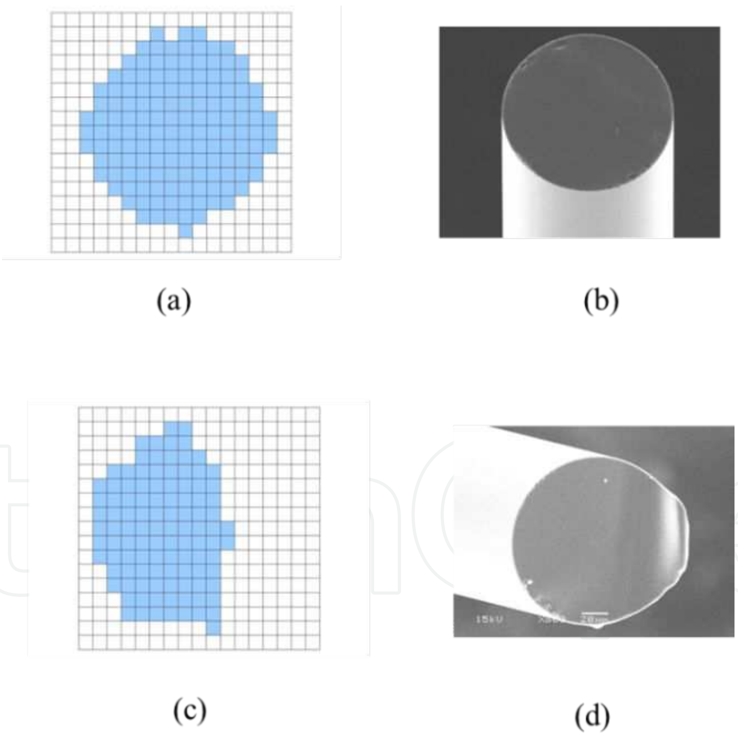

Figure 18. Experimental results of correctly cleaved fiber end: (a) result with proposed sensor and (b) result of SEM observation, and experimental results for incorrectly cleaved fiber end: (c) result with proposed sensor and (d) result of SEM observation

There are three important requirements for an inspection tool, namely it must provide a clear view, be portable, and easy to operate. We took these requirements into consideration when

http://dx.doi.org/10.5772/54241

developing the tool. For the clear view requirement, the fiber ends or connector endfaces under test should be viewable with both the naked eye and a camera. Naked-eye inspection is easily applicable and effective during fiber end preparation and assembly procedures. Camera inspection is effective because it allows us to photograph an inspected cleaved fiber end or connector endface. To meet the portability requirement, the tool must be compact and easy to carry to any location including aerial sites. For the ease of operation requirement, the tool should not require any focal adjustment of a microscope, and the tool must be as easy as possible to handle to prevent the need for complex operations in the field.

Several concrete specifications were determined on the basis of these requirements, as listed in Table 1. The tool must be small enough to carry with one hand. Its total weight should be less than 500 g. It should include a microscope that has a lens with a magnification power of a few hundred times. The target fiber is a 125-μm bare/250-μm coated fiber, which is placed in the FA holder used in field installable connectors or a holder for mechanical splicing. The target connectors are SC, MU, FA, and FAS connectors. The tool uses a cell phone equipped with a CCD camera and small video monitor. This enables the inspected fiber end to be photographed and sent over a cell phone network. LED light sources are used to allow visibility in dark places. A rechargeable battery is used for the LED light sources.

Description	Value/Comment
Size	Small enough to be carried with one hand
Weight	Less than 500 g
Microscope	Few hundred power magnification lens
Target fiber	125/250 (bare/coated) fiber in FA holder or holder for mechanical splicing
Target connector	SC, MU, FA, FAS connectors
Camera	Cell phone capable of taking photos
Light	LED
Battery	Rechargeable battery

Table 1. Specifications of new inspection tool

The tool is designed to inspect both cleaved fiber ends and connector endfaces. Schematic views of the inspection method for a cleaved fiber end and an optical connector endace are shown in Fig. 19(a) to (c). The fundamental optical microscope system for the tool is shown in Fig. 19(a). The microscope system is composed of an objective lens, an eyepiece lens for a cell phone camera or a naked eye, a sample that can be inspected, and an LED light source. Their components must be arranged in a line at designated lengths. In this figure, S_{ob}, L_a, S_{ey}, f_{ob}, and f_{ey} indicate the distance from the objective lens to the object point, the distance between the objective and eyepiece lenses, the distance from the eyepiece lens to the viewpoint for a cell phone camera or the naked eye, the focal distance of the objective lens, and the focal distance of the eyepiece lens, respectively. Here, S_{ob} is designed to be slightly larger than f_{ob}, and S_{ey} is designed to be slightly larger than f_{ey}. The figure also shows the light path. An LED light source emitting an almost parallel light beam, is used in this microscope system. After passing through the inspected sample, the light is focused at the back focal plane of the objective lens. It then proceeds to and is magnified by the eyepiece lens before passing into a cell phone camera or a naked eye. The magnified image of the inspected sample can be observed with the cell phone monitor or with the naked eye by using appropriate lenses and by designating appropriate distances; S_{ob}, L_a, and S_{ey}. With normal optical microscopes, the inspected sample is placed on the stage and must be adjusted to S_{ob} and aligned at the object point while L_a and S_{ey} are designated as constants. By contrast, with this microscope system, the inspected sample, which in placed in a special holder, can always be positioned at the object point without active alignment, i.e., without focal length adjustment. This special holder is described in detail in the following section. For the cleaved fiber inspection shown in Fig. 19(b), the side of the cleaved fiber end is designed to be viewed through the objective lens of the microscope system with the use of the LED light source. The distance between the fiber end and the objective lens a is designed to be equal to S_{ob}. The fiber end, LED, and lens are designed to align passively and to set at each designated distance and not require focal adjustment. However, for the optical-fiber connector inspection in Fig. 19(c), the endface of the connector is designed to be viewed through the objective lens by using a half-mirror and another LED light source. The summation of the distance between the connector endface and the half-mirror b and that between the half-mirror and the object lens c is designed to be equal to S_{ob}. The connector end, LED, half-mirror, and lens are also designed to align passively and to set at each designated distance and not require focal adjustment.

On the basis of the described specifications and design, we developed a simple, mobile and cost-effective tool. The outer components of the proposed inspection tool and the internal makeup of the optical microscope system are shown in Fig. 20. It is composed of three main parts: a body that includes a microscope that has objective and eyepiece lenses and LED light sources, a cell phone and its attachment, and special holders for cleaved fiber ends or connector endfaces. The cell phone is equipped with a CCD camera and a small video monitor. This inspection tool is simple and light, and weighs about 500 g including the cell phone. The optical microscope system is also shown in this figure. The eyepiece lens, objective lens, and object point of the cleaved fiber end are aligned in the body of the tool. The two LEDs for the cleaved fiber end and connector endface are also installed in the body. The half-mirror is aligned in the special holder for the connector endface. The inspection procedure is as follows.

i. The cleaved optical fiber or the optical connector to be inspected is placed in the appropriate special holder.

ii. The special holder is installed at the center of the body.

iii. The attachment with the cell phone is installed on top of the body.

The special holders and body are designed to automatically align the inspected cleaved fiber end or connector end at each of the object points after step (ii). The attachment for a cell phone is also designed to automatically align the camera in the cell phone at the viewpoint after step (iii). This structure and procedure result in the inspection tool not requiring focal adjustment.

The fiber ends or connector endfaces under test can be viewed through the top of the body (step ii) using the cell phone monitor (step iii).

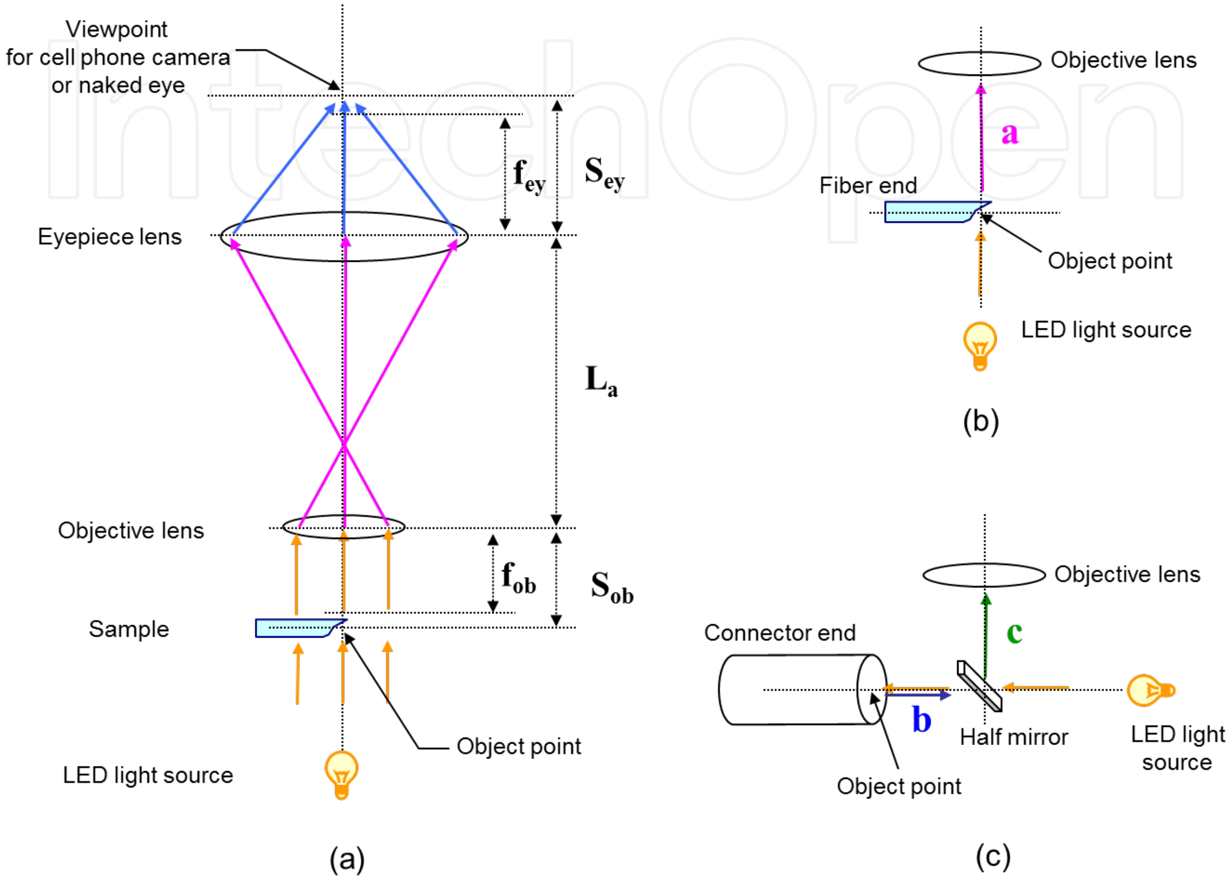

Figure 19. Basic concept of inspection method with developed tool: (a) fundamental optical microscope system and inspecting (b) cleaved fiber end (side) and (c) connector endface (front)

The conventional fiber end preparation procedure for an FAS connector has six steps: (1) cut the support wire of the dropped cable, (2) strip the cable coating, (3) place the fiber in the FA holder, (4) strip the fiber coating, (5) clean the stripped fiber (bare fiber) with alcohol, and (6) cut the bare optical fiber with a fiber cleaver. The assembly procedure comprises the next three steps: (7) insert the properly prepared bare optical fiber into the mechanical splice part in the FAS connector, (8) join it to the built-in optical fiber, and (9) fix the position of the bare optical fiber. The inspection procedure for the proposed inspection tool (i)-(iii) for a cleaved fiber end can be conducted between the fiber end preparation and assembly procedures, i.e., between steps (6) and (7). This indicates that the proposed inspection tool can work well with the conventional fiber end preparation and assembly procedures.

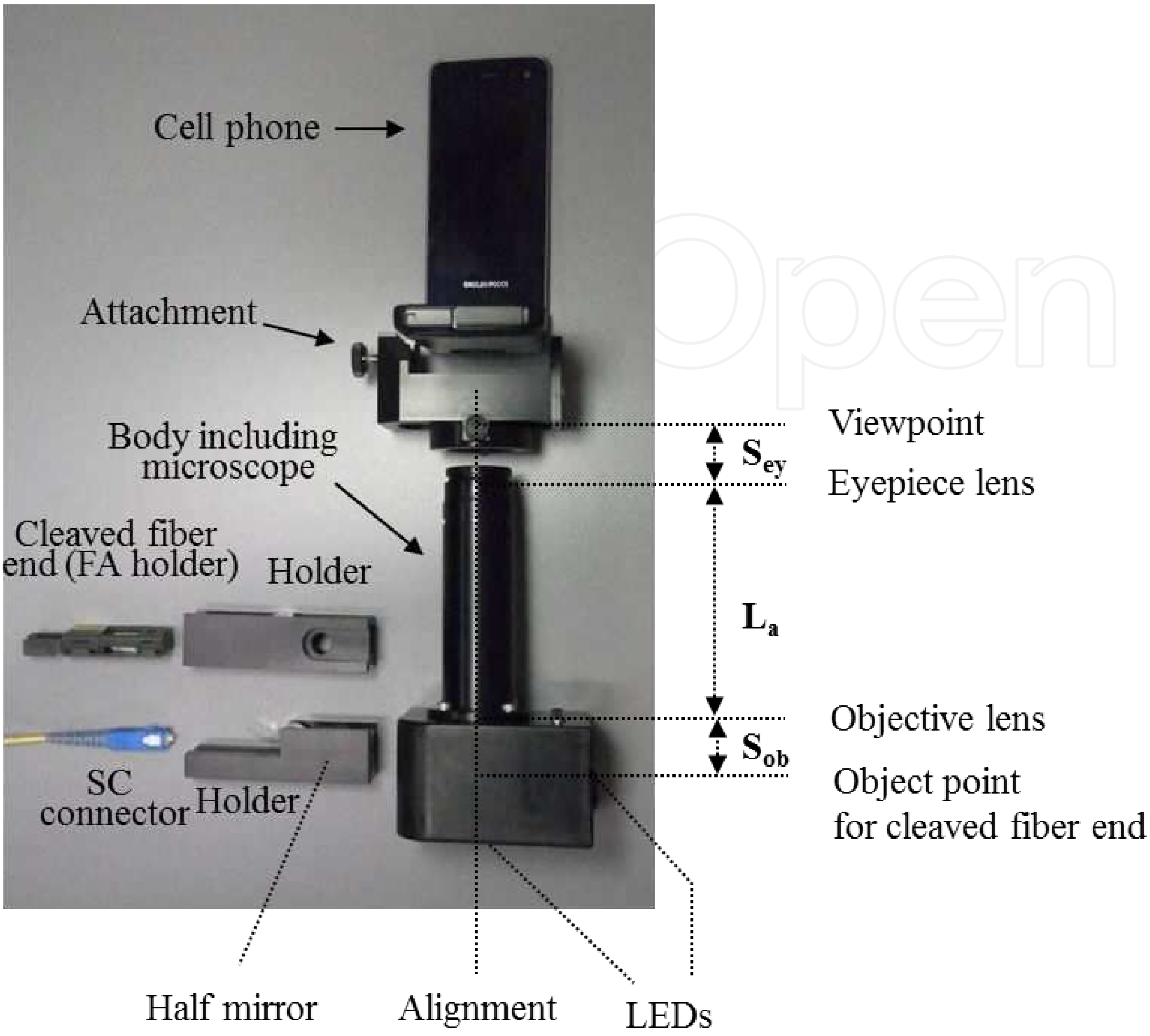

Figure 20. Outer components of fabricated inspection tool and internal makeup of optical microscope system

The inspection results and operation time of the fabricated inspection tool were evaluated. Experimental observation results from the cell phone screen are shown in Fig. 21. The tool with a cell phone attached is shown in Fig. 21(a), and its observation results are shown in Fig. 21(b) to (e). The fiber end or connector endface in each photo is magnified about 100 times. These results indicate that the tool can be used to inspect and determine whether fiber ends have been cleaved incorrectly (Fig. 21(b)) or correctly (Fig. 21(c)), and whether there is contamination (Fig. 21(d)) or no contamination (Fig. 21(e)) on the connector endfaces.

http://dx.doi.org/10.5772/54241

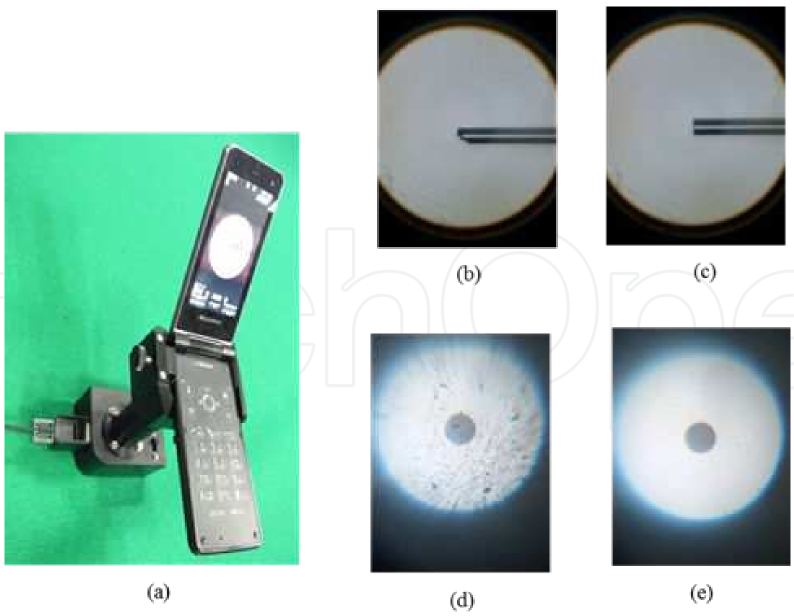

Figure 21. Experimental observation results on cell phone screen: (a) developed inspection tool with cell phone attached, (b) incorrectly cleaved fiber end, (c) correctly cleaved fiber end, (d) contamination on connector endface, and (e) uncontaminated connector endface

For conventional FAS connector procedures, the fiber end preparation and assembly procedures take 72 and 28% of the total installation time, respectively. With the proposed tool, inspection took 11% longer than with the conventional procedure. These results indicate that using the inspection tool may result in a slight increase of 11% in operation time compared with that required with conventional fiber end preparation and assembly procedures.

The fabricated inspection tool is compact, highly portable, and can inspect a fiber and clearly determine whether it has been cleaved correctly and whether contamination or scratches can be found on the connector endfaces. Thus, this tool will be highly practical for field use.

5. Conclusion

This chapter reported example faults and novel countermeasures with optical fiber connectors and mechanical splices in FTTH networks.

After a brief introduction (section 1), section 2 described the FTTH network and optical fiber connectors and mechanical splices used in Japan, and section 3 reported example faults with these optical connections in FTTH networks. First, the faults with fiber connection using refractive-index matching material were reported in section 3.1. There are two major causes of these faults: one is a wide gap between fiber ends and the other is incorrectly cleaved fiber ends. Next, faults with fiber connection using physical contact were explained in section 3.2. This fault might occur when the connector endfaces are contaminated. The characteristics of these faults were outlined.

Novel countermeasures against these above-mentioned faults were introduced in section 4. In section 4.1, a new connection method using solid refractive index matching material was proposed as a countermeasure against faults caused by the wide gap between fiber ends. This connection method can provide an insertion loss of more than 20 dB or less than 2 dB when the gap between the fiber ends is wider or narrower than 120 μm, respectively. If there is a defective connection that has a wide gap, the insertion loss will always be extremely high. In such cases, communication services may be immobilized. With the connection method, engineers undertaking detection work can notice the defective connection immediately after installation.

In section 4.2, a fiber optic Fabry-Perot interferometer-based sensor was introduced as a countermeasure for detecting faults caused by incorrectly cleaved fiber ends. The sensor mainly uses laser diodes, an optical power meter, a 3-dB coupler, and an XY lateral adjustment fiber stage. Experimentally obtained fiber end images were in good agreement with scanning electron microscope observation images of incorrectly cleaved fiber ends.

In section 4.3, a novel tool for inspecting optical fiber ends was proposed as a countermeasure for detecting faults caused both by incorrectly cleaved fiber ends and by contaminated connector endfaces. The proposed tool has a simple structure and does not require focal adjustment. It can be used to inspect a fiber and clearly determine whether it has been cleaved correctly and whether contamination or scratches are present on the connector endfaces. The tool requires a slight increase of 11% in operation time compared with conventional fiber end preparation and assembly procedures. The proposed tool provides a simple and cost-effective way of inspecting cleaved fiber ends and connector endfaces and is suitable for field use.

These results support the practical use of optical fiber connections in the construction and operation of optical network systems such as FTTH.

Acknowledgements

This work was supported by the TASC, NTT East Corporation, Japan. The author is deeply grateful to the following members of the TASC for their support; to Y. Yajima for discussing the experiments related to fiber connection with refractive index matching material, to H. Onose for discussing the experiments related to contaminated connector endfaces, to H. Watanabe and M. Tanaka for helpful discussions regarding the new connection method using solid refractive index matching material and a fiber optic Fabry-Perot interferometer based sensor, and to M. Okada and M. Hosoda for discussions regarding the simple inspection tool.

Author details

Mitsuru Kihara

NTT Access Network Service Systems Laboratories, Nippon Telegraph and Telephone Corporation, Japan

References

[1] Ministry of Internal Affairs and Communications, 2011 WHITE PAPER Information and Communications in Japan [online], Available at: http://www.soumu.go.jp/johotsusintokei/whitepaper/ja/h23/pdf/index.html (accessed 10 Aug. 2012).

[2] Matsuhashi K., Uchiyama Y., Kaiden T., Kihara M., Tanaka H., & Toyonaga M. "Fault cases and countermeasures against damage caused by wildlife to optical fiber cables in FTTH networks in Japan," in Proceeding of the 59th IWCS/Focus, Nov. 7-10, 2010, Providence, Rhode Island, USA, pp. 274-278.

[3] NTT East Corporation, "Fault cases and countermeasures for field assembly connectors in optical access facilities," NTT Technical Review, vol. 9, No. 7, 2011.

[4] Kihara M., Nagano R., Uchino M., Yuki Y., Sonoda H., Onose H., Izumita H., & Kuwaki N., "Analysis on performance deterioration of optical fiber joints with mixture of refractive index matching material and air-filled gaps," in Proceedings of the OFC/NFOEC, March 22-26, 2009, San Diego, CA, USA, JWA4.

[5] Kihara M., Uchino M., Watanabe H., & Toyonaga M., "Fault analysis: optical performance investigation of optical fiber connections with imperfect physical contact," Opt. Lett., vol. 36, no. 24, 2011, pp. 4791-4793.

[6] Kihara M., "Optical performance analysis of single-mode fiber connections," in the book "Optical fiber communications and devices" edited by Moh. Yasin, Sulaiman W. Harun and Hamzah Arof, ISBN 978-953-307-954-7, InTech, February 2, 2012.

[7] Nakajima T., Terakawa K., Toyonaga M., & Kama M., "Development of optical connector to achieve large-scale optical network construction," in Proceedings of the 55th IWCS/Focus, Nov. 12-15, 2006, Providence, Rhode Island, USA, pp. 439–443.

[8] Hogari K., Nagase R., & Takamizawa K., "Optical connector technologies for optical access networks," IEICE Trans. Electron., Vol. E93-C, No. 7, 2010, pp. 1172–1179.

[9] Sugita E., Nagase R., Kanayama K., & Shintaku T., "SC-type single-mode optical fiber connectors," IEEE/OSA J. Lightw. Technol., vol. 7, 1989, pp. 1689–1696.

[10] Nagase R., Sugita E., Iwano S., Kanayama K., & Ando Y., "Miniature optical connector with small zirconia ferrule," IEEE Photon. Technol. Lett., vol. 3, No. 11, 1991, pp. 1045–1047.

[11] "Optical fiber mechanical splice", US patent No.5963699.

[12] Satake T., Nagasawa S., & Arioka R., "A new type of a demountable plastic molded single mode multifiber connector," IEEE/OSA J. Lightw. Technol., vol. LT-4, 1986, pp. 1232-1236.

[13] Kihara M., Nagano R., Izumita H., & Toyonaga M., "Unusual fault detection and loss analysis in optical fiber connections with refractive index matching material," Optical Fiber Technol., vol. 18, 2012, pp. 167–175.

[14] Yajima Y., Watanabe H., Kihara M., & Toyonaga M., "Optical performance of field assembly connectors using incorrectly cleaved fiber ends," in Proceedings of the OECC2011, July 4-8, 2011, Kaohsiung, Taiwan, 7P3_053.

[15] Berdinskikh T., Bragg J., Tse E., Daniel J., Arrowsmith P., Fisenko A., & Mahmoud S., "The contamination of fiber optics connectors and their effect on optical performance," in Technical digest series of OFC 2002, March 17- 22, 2002, Anaheim, California, pp. 617-618.

[16] Albeanu N., Aseere L., Berdinskikh T., Nguyen J., Pradieu Y., Silmser D., Tkalec H., & Tse E., "Optical connector contamination and its influence on optical signal performance," J SMTA, vol. 16, issue 3, 2003, pp. 40-49.

[17] Berdinskikh T., Chen J., Culbert J., Fisher D., Huang S. Y., Roche B. J., Tkalec H., Wilson D., & Ainley S. B., "Accumulation of particles near the core during repetitive fiber connector matings and de-matings" in Technical Digest of OFC/NFOEC2007, March 25-29, 2007, Anaheim, CA, USA, NThA6, pp. 1-11.

[18] Marcuse D., "Loss analysis of optical fiber splice," Bell Sys. Tech. J, vol. 56, 1976, pp. 703-718.

[19] Kihara M., Nagasawa S., & Tanifuji T., "Return loss characteristics of optical fiber connectors," IEEE/OSA J. Lightw. Technol., vol. 14, Sep. 1996, pp. 1986-1991.

[20] For example, CLETOP (Optical connector cleaner), see URL: http://www.ntt-at.com/product/cletop/

[21] Tanaka M., Watanabe H., Kihara M., & Takaya M., "New connection method using solid refractive index matching material," in Proceedings of the OECC2012, July 2-6, 2012, Busan, Korea, 4C2-5.

[22] Tanifuji T., Kato Y., & Seikai S., "Realization of a low-loss splice for single-mode fibers in the field using an automatic arc-fusion splicing machine," in Proceedings of the OFC, Feb. 28-March 2, 1983, New Orleans, Louisiana, USA, MG3.

[23] Kihara M., Watanabe H., Tanaka M., & Toyonaga M., "Fiber optic Fabry-Perot interferometer based sensor for inspecting cleaved fiber ends," Microwave and Optical Technol. Lett., vol. 54, No. 6, 2012, 1541-1543.

[24] Watanabe H., Kihara M., Tanaka M., & Toyonaga M., "Inspection technique for cleaved optical fiber ends based on Fabry-Perot interferometer," IEEE/OSA J. Lightw. Technol., vol. 30, No. 8, 2012, 1244-1249.

[25] Yariv A., "Introduction to optical electronics," New York: Holt, Rinehart, and Winstone, 1985.

[26] Kashima N., "Passive optical components for optical fiber transmission," Norwood, MA: Artech House, 1995.

[27] Kihara M., Tomita S., & Haibara T., "Influence of wavelength and temperature changes on optical performance of fiber connections with small gap," IEEE Photon. Tech. Lett. 18, 2006, 2120-2122.

[28] Kihara M., Uchino M., Omachi M., & Izumita H., "Analyzing return loss deterioration of optical fiber joints with various air-filled gaps over a wide wavelength range," in Proceedings of the OFC/NFOEC, March 21-25, 2010, San Diego, CA, USA, NWE4.

[29] For example, JDSU Fiberscope (Fiber Optic Connector End Face Cleaning System), see URL: http://www.jdsu.com/en-us/Test-and-Measurement/Products/families/westover/Pages/default.aspx/

[30] Okada M., Kihara M., Hosoda M., &Toyonaga M., "Simple inspection tool for cleaved optical fiber ends and optical fiber connector end surface," in Proceedings of the 60th IWCS, Nov. 7-9, Charlotte, North Carolina, USA, 2011, 270-274.

[31] Kihara M., Okada M., Hosoda M., Iwata T., Yajima Y., & Toyonaga M., "Tool for inspecting faults from incorrectly cleaved fiber ends and contaminated optical fiber connector end surfaces," Optical Fiber Technol., vol. 18, 2012, 470-479.